Progress of Theoretical Physics, Vol. 112, No. 4, October 2004

Relativistic Hartree-Bogoliubov Calculation of the Specific Heat for the Inner Crust of Neutron Stars

Takuya NAKANO[1,*] and Masayuki MATSUZAKI[2,**]

[1]*Department of Physics, Kyushu University, Fukuoka 812-8581, Japan*
[2]*Department of Physics, Fukuoka University of Education, Munakata 811-4192, Japan*

(Received July 7, 2004)

We calculate the specific heat of the inner crust of neutron stars, which determines the cooling time, using a local-density approximation of an improved relativistic Hartree-Bogoliubov model. The non-uniformity of the system enhances the specific heat, especially at low temperatures. We examine a schematic interpolation between the results of Broglia et al., adopting the Gogny force, and ours, based on the Lagrangian of the relativistic mean-field model.

§1. Introduction

The inner crust of a neutron star, with densities ranging from the neutron drip density to values of the order of the saturation density, is a non-uniform system consisting of a Coulomb lattice of neutron-rich nuclei and a sea of free neutrons. In this layer, free neutrons exist in the form of a $^1S_0$ superfluid. This layer conveys a drop in temperature due to neutrino emission in the core to the surface. The rate of the conveyance depends on the specific heat and the thickness of the inner crust. The dependence of the cooling (random walk) time of young neutron stars, $t_{\rm rw}$, on these quantities is studied in Ref. 1). There, it is found that $t_{\rm rw} \simeq L^2/D$, where L is the thickness of the inner crust and D is the diffusivity. The latter is given by dividing the thermal conductivity by the specific heat.[2)] This relation implies a linear dependence of the cooling time on the specific heat. Later, the investigation reported in Ref. 3) confirmed this relation approximately with a numerical simulation, although the effect of the superfluidity on the specific heat was not included there.

Reference 4) first studied the effect of superfluidity on the specific heat of a non-uniform inner crust using the Gogny force, which has the characteristic that superfluidity survives up to a rather high density. Because superfluidity reduces the specific heat, it leads to a decrease of $t_{\rm rw}$. More specifically, it causes a shortening of the length of the early plateau in the cooling curve.[5)] Here, we study such a non-uniform system, adopting the RMF interaction. This interaction has the property that the superfluid gap closes at a lower density. It is a one-boson exchange interaction derived from the Lagrangian density of the relativistic mean field (RMF) model with a momentum cutoff. We call the RMF model with a pairing field the "relativistic Hartree-Bogoliubov model" and that with a momentum cutoff in the

*) Present Address: Sasaguri Town Office, Sasaguri, Fukuoka 811-2492, Japan
**) Corresponding author, E-mail: matsuza@fukuoka-edu.ac.jp

pairing channel the "improved relativistic Hartree-Bogoliubov model". As a first step of this application, we adopt a local-density approximation and ignore possible non-spherical shapes of neutron-rich nuclei.

§2. The model

We begin with the simplest version of the RMF model, the σ-ω model. Its Lagrangian density reads

$$\begin{aligned}\mathcal{L} =&\bar{\psi}(i\gamma_\mu\partial^\mu - M)\psi \\ &+\frac{1}{2}(\partial_\mu\sigma)(\partial^\mu\sigma) - \frac{1}{2}m_\sigma^2\sigma^2 - \frac{1}{4}\Omega_{\mu\nu}\Omega^{\mu\nu} + \frac{1}{2}m_\omega^2\omega_\mu\omega^\mu \\ &+g_\sigma\bar{\psi}\sigma\psi - g_\omega\bar{\psi}\gamma_\mu\omega^\mu\psi, \\ \Omega_{\mu\nu}=&\,\partial_\mu\omega_\nu - \partial_\nu\omega_\mu. \end{aligned} \tag{1}$$

Here ψ, σ and ω denote the neutron, the sigma boson and the omega meson, respectively. Their masses are $M = 939$ MeV, $m_\sigma = 550$ MeV and $m_\omega = 783$ MeV. The coupling constants are $g_\sigma^2 = 91.64$ and $g_\omega^2 = 136.2$, as given in Ref. 6). Solving the equations of motion derived from $\mathcal{L}$ with the mean field approximation for σ and ω, we obtain the single-particle spectrum $E(k)$ (whose explicit form is given later) of ordinary (normal fluid) pure neutron matter. The RMF pairing interaction is also derived from this $\mathcal{L}$ as

$$\bar{v}(\boldsymbol{p},\boldsymbol{k}) = \langle \boldsymbol{p}s', \tilde{\boldsymbol{p}s'}|V|\boldsymbol{k}s, \tilde{\boldsymbol{k}s}\rangle - \langle \boldsymbol{p}s', \tilde{\boldsymbol{p}s'}|V|\tilde{\boldsymbol{k}s}, \boldsymbol{k}s\rangle, \tag{2}$$

with the tildes denoting time reversal. Here, V represents the σ and ω exchange between neutrons (the second-order diagram of the coupling terms). Integration over the angle between $\boldsymbol{p}$ and $\boldsymbol{k}$ to project out the S wave component gives $\bar{v}(p,k)$.

The first attempt to describe superfluidity in uniform infinite nuclear matter adopting the RMF interaction is given in Ref. 7). However, the result obtained there is not very realistic, in that the resulting pairing gap is too large. This can be attributed to unphysical behavior of the RMF interaction at high momenta; i.e., the repulsion is too strong. The ${}^1S_0$ pairing gap Δ in infinite matter is obtained by solving the gap equation,

$$\Delta(k_{\rm F}) = -\frac{1}{8\pi^2}\int_0^\infty \bar{v}(k_{\rm F},k)\frac{\Delta(k)}{\sqrt{(E(k)-E(k_{\rm F}))^2+\Delta^2(k)}}k^2dk\,. \tag{3}$$

This equation indicates that primarily attraction [$\bar{v}(k_{\rm F},k) < 0$] brings about the relation $\Delta(k_{\rm F}) > 0$. However, repulsion [$\bar{v}(k_{\rm F},k) > 0$] can also do this if $\Delta(k) < 0$. Qualitatively, this actually occurs at high k, irrespective of whether the RMF interaction constructed for the description of the finite density system or the bare interaction that reproduces the nucleon-nucleon scattering in the free space is adopted. Quantitatively, this contribution is too large in the calculation of Ref. 7) mentioned above. Then, the simplest way to reduce pairing gap is to cut off the momentum integration in Eq. (3) at an appropriate value $k = \Lambda$. Tanigawa and one of the

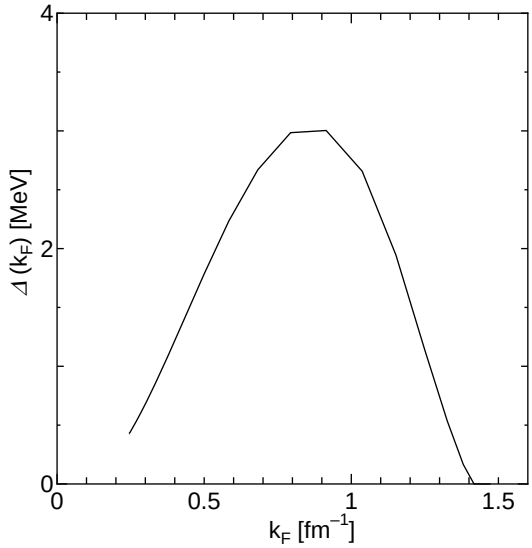

Fig. 1. Pairing gap at the Fermi surface of neutron matter as a function of the Fermi momentum [$\propto$ (density)$^{1/3}$]. This graph was calculated using the cutoff parameter $\Lambda = 3.60$ fm^{-1}.

present authors proposed a method to determine a density-independent cutoff parameter Λ quantitatively.[8] In that work, the optimal value of Λ was determined for symmetric nuclear matter, because the original parameters of the RMF model were adjusted for it. In the present work, the same value of Λ is used for neutron matter. The result is plotted in Fig. 1. In this calculation, not only is the maximum gap reduced, but also the gap is made to close at a lower $k_{\rm F}$ by introducing Λ. Although a more sophisticated way to modulate the high-momentum part smoothly was also developed later in Ref. 9), the simple method presented in Ref. 8) is sufficient for the present purpose, since only the pairing gap at the Fermi surface at each density is necessary in a local-density approximation.

In order to describe a non-uniform system composed of a lattice of neutron-rich nuclei and a sea of free neutrons, we adopt the Wigner-Seitz (WS) approximation, in which each spherical cell contains at its center one nucleus permeated by free neutrons that have dripped off from it. We parametrize the neutron density obtained from a density-dependent Hartree-Fock calculation in Ref. 10) in terms of the Woods-Saxon form

$$\rho_{\rm n}(r) = \frac{\rho_{0,\rm n}}{1+\exp[(r-R_{\rm n})/a_{\rm n}]} + \rho_{\rm ext,n}\,, \tag{4}$$

as done in Ref. 4). We carried out calculations at five representative densities in accordance with that work. The parameters used in Eq. (4) are listed in Table I. The radii of the WS cells are also included. Here we introduce a local-density approximation; that is, we assume a uniform Fermi gas of neutrons at each spatial point. Then the local Fermi momentum is calculated from the local density given by Eq. (4) as

$$k_{\rm F}(r) = (3\pi^2\rho_{\rm n}(r))^{1/3}\,. \tag{5}$$

Table I. Parameters used in Eq. (4) and the radii of the Wigner-Seitz cells.

	ρ/ρ_0	$\rho_{0,\mathrm{n}}$ (fm^{-3})	$\rho_{\mathrm{ext,n}}$ (fm^{-3})	R_{n} (fm)	a_{n} (fm)	R_{ws} (fm)
A	0.46	0.114	0.0737	5.0	1.2	15.0
B	0.28	0.101	0.0436	7.0	1.1	20.9
C	0.12	0.098	0.0184	7.4	0.8	29.4
D	0.034	0.104	0.0047	6.8	0.9	35.5
E	0.005	0.108	0.0005	5.9	0.9	45.7

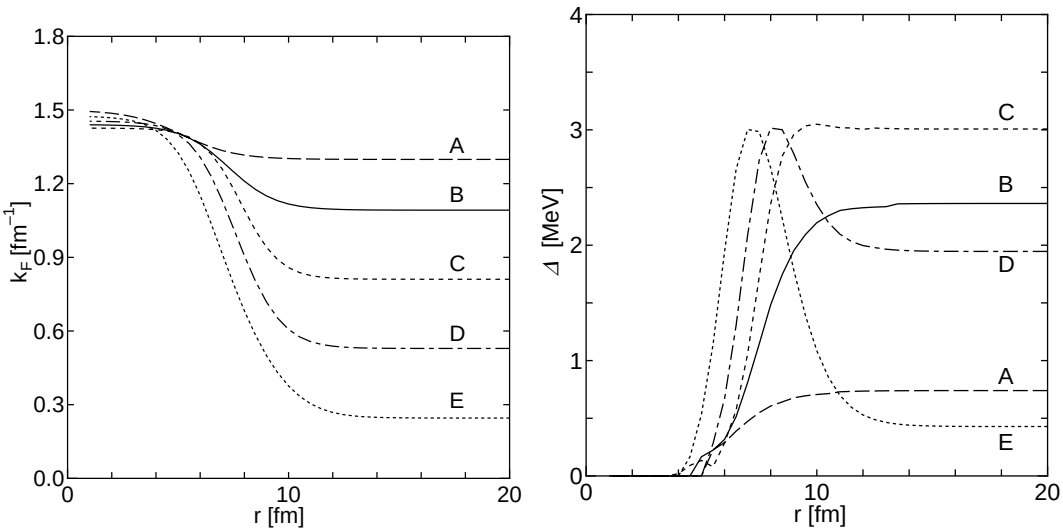

Fig. 2. Profile of the local Fermi momentum (left) and of the local pairing gap (right) in a Wigner-Seitz cell.

The profile of this momentum in each WS cell is plotted in the left panel of Fig. 2. This determines the profile of the pairing gap, because the gap in uniform neutron matter is calculated as a function of k_{F}, as shown in Fig. 1. The resulting $\Delta(r, k_{\mathrm{F}}(r))$ is displayed in the right panel of Fig. 2, whereas $\Delta(r,p)$ at every r and p is needed for the local quasi-particle energy,

$$\mathcal{E}(r,p) = ((E(p) - E(k_{\mathrm{F}}(r)))^2 + \Delta^2(r,p))^{1/2} . \tag{6}$$

Here, $E(p) = (p^2+M^{*2})^{1/2}+g_\omega\langle\omega^0\rangle$ is the single-particle energy, and $M^* = M-g_\sigma\langle\sigma\rangle$ is the density-dependent effective neutron mass. In these expressions, $\langle\cdot\rangle$ represents the expectation value of the indicated boson field. Note that M^* is calculated in pure neutron matter, not in β-equilibrated neutron star matter, while the electron contribution to the specific heat is taken into account below.

Now we are ready to calculate the specific heat of the system. The specific heat is calculated from the entropy,

$$S = -2\int d^3r \int \frac{d^3p}{(2\pi)^3} \left\{ f(r,p)\ln f(r,p) + [1-f(r,p)]\ln[1-f(r,p)] \right\} , \tag{7}$$

as

$$C_{V\mathrm{n}} = T\frac{\partial S}{\partial T}\bigg|_{V} . \tag{8}$$

The phase-space distribution function in Eq. (7) is

$$f(r,p) = \frac{1}{1+\exp[\mathcal{E}(r,p)/T]} , \tag{9}$$

where the quasi-particle energy is given by Eq. (6). The final expression is

$$C_{V\mathrm{n}} = \frac{1}{\pi T^2 V_{\mathrm{ws}}} \int_{V_{\mathrm{ws}}} dr\, r^2 \int dp\, p^2 \frac{\mathcal{E}^2(r,p)}{\cosh^2[\mathcal{E}(r,p)/2T]} . \tag{10}$$

The spatial integration is performed over each WS cell, and the momentum integration is done up to $\Lambda = 3.60$ fm^{-1}, determined in Ref. 8) to give physical pairing gaps. Note that the temperature dependence of the quasi-particle energy is ignored, because only low temperatures are of interest in the present study. In addition to neutrons, a degenerate electron gas, which we assume to be uniform, gives a comparable contribution,[11)]

$$C_{V\mathrm{e}} = \frac{1}{3} k_{\mathrm{F}}^2 (m^2 + k_{\mathrm{F}}^2)^{1/2} T , \tag{11}$$

while that from protons is negligible.[4)] This expression indicates that, because of the equilibrium of the chemical potential, the electron contribution increases as the density increases. Thus, the total specific heat is given by

$$C_{V\mathrm{tot}} = C_{V\mathrm{n}} + C_{V\mathrm{e}} . \tag{12}$$

§3. Results and discussion

The effect of non-uniformity can be seen by comparing the upper-left (showing $C_{V\mathrm{n}}$ for uniform matter) and the upper-right (for non-uniform) panels of Fig. 3. One characteristic is that the density dependence is weak in the non-uniform system. This is due to a density-dependent increase of $C_{V\mathrm{n}}$. The reason why non-uniformity causes $C_{V\mathrm{n}}$ to increase can be inferred from an expression obtained using a weak-coupling approximation for the uniform system,[12)]

$$\frac{C_{V\mathrm{n}}}{T} \propto \left(\frac{\Delta_0}{T}\right)^{5/2} \exp\left(-\frac{\Delta_0}{T}\right) , \tag{13}$$

with Δ_0 being the uniform gap. This is a decreasing function of Δ_0/T at low temperatures, specifically, for $\Delta_0/T > 5/2$, and consequently leads to $C_{V\mathrm{n}}(\mathrm{normal}) > C_{V\mathrm{n}}(\mathrm{super})$. Since non-uniformity produces a region where the gap is small, it results in an increase of $C_{V\mathrm{n}}$. This effect is in particular conspicuous at lower temperatures, because a small variation in Δ_0 leads to a large variation in Δ_0/T. Contrastingly, the difference in Δ_0 is not important at high temperatures.

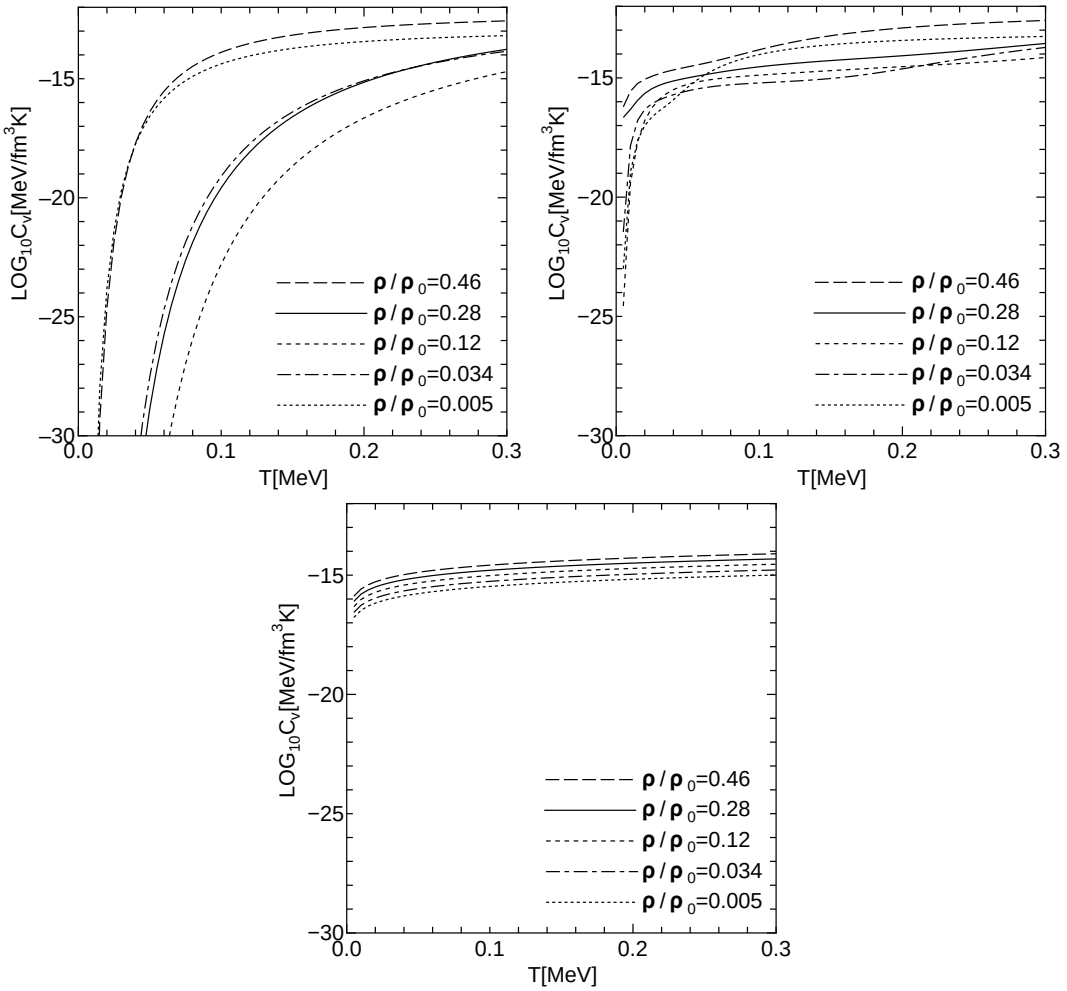

Fig. 3. Temperature dependence of the partial specific heat of uniform neutrons (upper-left), non-uniform neutrons (upper-right) and electrons (lower). Note that, because the critical temperature is estimated with a weak-coupling formula as $T_{\rm c} = \Delta_0/1.76$,[12] the temperature region considered here is well below it (see Fig. 2).

Because the contribution from electrons is of the same order (the lower panel of Fig. 3) as that from the non-uniform neutrons, the enhancement of $C_{V\rm tot}$,

$$\frac{C_{V\rm tot}({\rm nu})}{C_{V\rm tot}({\rm u})} = \frac{C_{V\rm n}({\rm nu}) + C_{V\rm e}}{C_{V\rm n}({\rm u}) + C_{V\rm e}}\,, \tag{14}$$

where "nu" and "u" indicate non-uniform and uniform, is in the neighborhood of 3 to 4, as shown in Fig. 4. Comparing this to Fig. 3 in Ref. 4) elucidates the difference at low temperatures. This difference leads to that in the cooling time. The considerations above indicate that the difference originates from the region where the pairing gap is small — the interior region of the nucleus at the center of the WS cell. Actually, although the Gogny force adopted in Ref. 4) is known to yield pairing

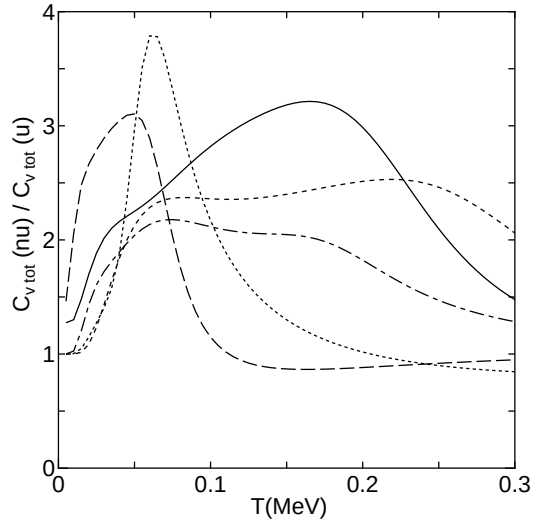

Fig. 4. Temperature dependence of the ratio of the total specific heats. The legend of the curves is the same as in Fig. 3.

properties similar to those given by bare interactions at low densities,[13] there is the big difference at high densities that the superfluid phase survives far above the saturation density (see Fig. 5.4 of Ref. 14) and Fig. 3 of Ref. 15), for example). In contrast, our cutoff parameter in the RMF description was determined so as to reproduce the pairing properties given by one of the bare interactions, the Bonn-B potential, and accordingly, the pairing gap closes near the saturation density. (See Fig. 2(a) of Ref. 8) for the symmetric matter case.) This makes the gap in the interior region vanish. In Ref. 16), the non-relativistic version of the Bonn-A potential is adopted, and the results for $\rho/\rho_0 = 0.058$ and 0.176, where a spherical shape is expected for neutron-rich nuclei, are presented. Our results for the cases B, C and D in Table I are very similar to theirs with respect to the heights and the T dependences. Here, one comment is in order concerning the double-counting problem for short-range correlations, which arises when effective interactions are adopted in the gap equation. In principle, this problem does exist, as pointed out in Ref. 16), but the analysis given in Ref. 9) indicates that it does not significantly affect the results.

Since the essential difference between the results given in Ref. 4) and ours regards the gap in the interior region, as mentioned above, we examine a schematic interpolation between the two models; we vary the gap in this region by hand, as shown in the upper-left panel of Fig. 5 for the density of case B in Table I. The resulting specific heats are presented in the upper-right panel. Clearly, $C_{V\mathrm{n}}$ approaches that given in Ref. 4) (see Fig. 2 therein) as the gap in the interior region is increased and to that of uniform matter by further increase. Finally, the ratio of the total specific heats is shown in the lower panel. This confirms that the vanishing gap in the interior region is the cause of the enhancement of $C_{V\mathrm{tot}}$ at low temperatures.

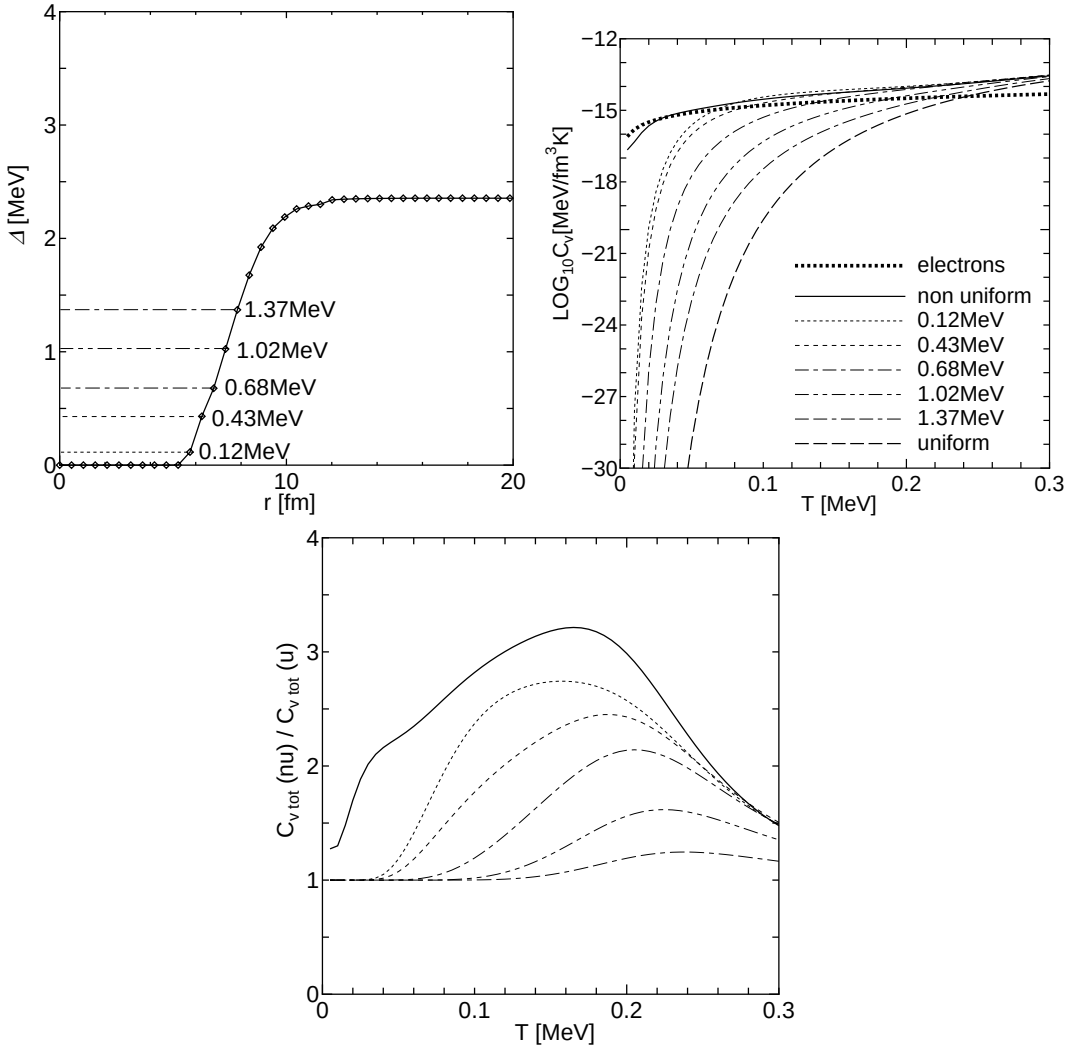

Fig. 5. Schematic variation of the gap profile (upper-left), the resulting temperature dependence of the neutron specific heat (upper-right), and that of the ratio of the total specific heats (lower). Here, we consider the density of case B in Table I.

§4. Concluding remarks

We have calculated the specific heat of the inner crust of neutron stars. This work is in a sense a relativistic counterpart of Ref. 4). But more important than the difference between relativistic and non-relativistic is the difference in the pairing gap at high densities. In addition to the enhancement of the specific heat in comparison to the uniform case, treated in Ref. 4), our calculation yields a conspicuous enhancement at low temperatures, due to the suppression of the gap at high densities. Because the cooling time of young neutron stars depends linearly on the specific heat of the inner crust, the obtained enhancement leads to a direct effect on the cooling time.

Beyond this first-step calculation, two kinds of refinements are in order; one is to take into account non-spherical shapes of lattice nuclei in the high-density part of the inner crust, and the other is the so-called proximity effect beyond the local-density approximation, that is, the spread of the pair wave function measured by the coherence length. (See Fig. 2(b) of Ref. 8) for the symmetric matter case. Coherence lengths for neutron matter are somewhat smaller.) The former is examined in Refs. 16)–18), where it is shown to strengthen non-uniformity, whereas the latter has been shown to weaken it.[19)]

References

1) G. E. Brown, K. Kubodera, D. Page and P. Pizzochero, Phys. Rev. D **37** (1988), 2042.
2) C. Kittel and H. Kroemer, *Thermal Physics*, 2nd ed. (W. H. Freeman and Company, San Francisco and London, 1980).
3) J. M. Lattimer, K. A. Van Riper, M. Prakash and M. Prakash, Astrophys. J. **425** (1994), 802.
4) R. A. Broglia, F. De Blasio, G. Lazzari, M. Lazzari and P. M. Pizzochero, Phys. Rev. D **50** (1994), 4781.
5) D. Page, in *The Many Faces of Neutron Stars*, ed. R. Bucheri, J. van Paradijs and M. A. Alpar (Kluwer Academic Publishers, Dordrecht, 1998), p. 539.
6) B. D. Serot and J. D. Walecka, Adv. Nucl. Phys. **16** (1986), 1.
7) H. Kucharek and P. Ring, Z. Phys. A **339** (1991), 23.
8) T. Tanigawa and M. Matsuzaki, Prog. Theor. Phys. **102** (1999), 897.
9) M. Matsuzaki and T. Tanigawa, Nucl. Phys. A **683** (2001), 406.
10) J. W. Negele and D. Vautherin, Nucl. Phys. A **207** (1973), 298.
11) L. D. Landau and E. M. Lifschitz, *Statistical Physics*, 3rd edition (Butterworth-Heinemann, Oxford, 1980).
12) A. L. Fetter and J. D. Walecka, *Quantum Theory of Many-Particle Systems* (McGraw-Hill, New-York, 1971).
13) G. F. Bertsch and H. Esbensen, Ann. of Phys. **209** (1991), 327.
14) P. Ring, Prog. Part. Nucl. Phys. **37** (1996), 193.
15) E. Garrido, P. Sarriguren, E. Moya de Guerra and P. Schuck, Phys. Rev. C **60** (1999), 064312.
16) Ø. Elgarøy, L. Engvik, E. Osnes, F. V. De Blasio, M. Hjorth-Jensen and G. Lazzari, Phys. Rev. D **54** (1996), 1848.
17) F. V. De Blasio and G. Lazzari, Phys. Rev. C **52** (1995), 418.
18) F. De Blasio, G. Lazzari, P. M. Pizzochero and R. A. Broglia, Phys. Rev. D **53** (1996), 4226.
19) F. Barranco, R. A. Broglia, H. Esbensen and E. Vigezzi, Phys. Rev. C **58** (1998), 1257.